



Shark eggs contribute to the trophic ecology of a cold-seep chemosynthetic ecosystem

Tal Zvi-Kedem^{1,2}, Stephane Martinez³, Eli Shemesh¹, Maya Lalzar⁴,
Tamar Guy-Haim^{2,5}, Guy Sisma-Ventura², Yizhaq Makovsky^{6,7}, Dan Tchernov¹,
Maxim Rubin-Blum^{2,8,*}

¹Morris Kahn Marine Research Station, Department of Marine Biology, Charney School of Marine Sciences, University of Haifa, Haifa 3498838, Israel

²Israel Oceanographic and Limnological Research, Tel-Shikmona, PO Box 9753, Haifa 3109701, Israel

³Graduate School of Oceanography, University of Rhode Island, Narragansett, RI 02882, USA

⁴Bioinformatics Services Unit, University of Haifa, Haifa 3498838, Israel

⁵Department of Life Sciences, Ben-Gurion University of the Negev, Beer Sheva 84105, Israel

⁶The Dr. Moses Strauss Department of Marine Geosciences, Charney School of Marine Sciences, University of Haifa, Haifa 3498838, Israel

⁷The Hatter Department of Marine Technologies, Charney School of Marine Sciences, University of Haifa, Haifa 3498838, Israel

⁸Department of Marine Biology, Charney School of Marine Sciences, University of Haifa, Haifa 3498838, Israel

ABSTRACT: Cold seeps host oasis-type ecosystems sustained by microorganisms such as chemosymbiotic bacteria, fueled by reduced gasses like hydrogen sulfide and methane. These habitats are characterized by a wealth of carbon and nutrient sources, substantial microbial turnover of key nutrients, and unknown metabolic interactions between symbionts and their hosts. Thus, the trophic ecology of cold seeps is not fully understood. Recent discoveries of massive shark nurseries and extensive chemotones in the southeastern Mediterranean Sea (SEMS) hint at a previously unknown complexity of food webs in this habitat. To provide insights into the trophic ecology of SEMS seeps, we collected symbiont-bearing (*Lamellibrachia anaximandri* tubeworms, *Idas modiolaeformis* mussels, and *Lucinoma kazani* clams) and other fauna, such as eggs of *Galeus melastomus* sharks, *Gracilechinus elegans* echinoids, *Clelandella myriamae* gastropods, and *Calliax lobata* ghost shrimps, from the Palmahim Disturbance seeps (~1000–1150 m water depth, Levantine basin in the SEMS). We obtained bulk and compound-specific values ($\delta^{13}\text{C}$ and $\delta^{15}\text{N}$), using isotope ratio mass spectrometry and compound-specific isotopic analysis of amino acids. Glutamic-acid–phenylalanine trophic position ($\text{TP}_{\text{Glu-Phe}}$) and the contribution of reworked organic matter (microbial resynthesis index, ΣV) were estimated for individual specimens. Our findings indicate a wealth of nutrition strategies and trophic interactions, as chemosynthetic productivity and external sources sustain these communities. Collagen-rich eggs of *G. melastomus* appear to sustain the opportunistic detritivores/carnivores such as *G. elegans* (maximum $\text{TP}_{\text{Glu/Phe}} = 4.7$; higher than that of *G. melastomus*, maximum $\text{TP}_{\text{Glu/Phe}} = 3.8$), but also supplement the chemosynthetic nutrition of *Idas* mussels, likely through heterotrophic symbionts.

KEY WORDS: Cold seep · Food web · Trophic position · Compound-specific amino acid analysis · $\delta^{13}\text{C}$ · $\delta^{15}\text{N}$ · Chemosynthesis · Resynthesis

1. INTRODUCTION

Cold seeps are widespread from the tropics to the poles, and at depths ranging from shallow shelf areas to the deep sea (Olu-Le Roy et al. 2004, Pop Ristova

et al. 2015, Joye 2020, Åström et al. 2022). These oases of life in the deep sea typically form dense macrofaunal communities, fueled by the seabed discharge of energy-rich gases, such as methane and hydrogen sulfide (Levin 2005, Jørgensen & Boetius

*Corresponding author: mrubin@ocean.org.il

2007, Duperron 2010). Food webs in seep ecosystems are largely based on productivity by chemosynthetic microbes that use these energy sources to assimilate carbon and nutrients into their biomass (Levin 2005). Various invertebrates, such as siboglinid tubeworms, bathymodioline mussels, and vesicomid and lucinid clams, flourish in seeps owing to nutritional symbioses with chemosynthetic microbes (Sogin et al. 2021). These organisms are seep ecosystem engineers that increase the complexity of these habitats, supporting other taxa (Levin 2005). The patchy distribution of these foundation species along physico-chemical gradients underpins the spatial heterogeneity of seep ecosystems (Levin et al. 2005, Portail et al. 2016).

Seep food webs are usually structured by weak trophic links among co-occurring species, with limited direct predation (Cordes et al. 2010, Portail et al. 2016). Apart from chemosynthetic fauna, trophic guilds can include bacterivorous/archivorous specialists, detritivores, and predators (Carlier et al. 2010, Portail et al. 2016, Åström et al. 2019, 2022). These food webs may not rely on chemosynthetic productivity alone, with inputs of photosynthetically derived material (Carlier et al. 2010, Vokhshoori et al. 2021, Åström et al. 2022) and reworking of seep organic matter (Morganti et al. 2022). Migrant organisms may feed in seep ecosystems, exporting seep carbon (MacAvoy et al. 2002, Olu et al. 2009, Portail et al. 2016). Among these migrant organisms, blackmouth catsharks *Galeus melastomus* lay their collagen-rich eggs (Rusaouën et al. 1976) in seeps, potentially adding biomass and detritus (Treude et al. 2011). This may imply not only export but also result in unexpected inputs of organics by migrants into seep food webs.

Here we aimed to elucidate the trophic ecology of chemosynthetic communities that are associated with hydrocarbon seeps and brine pools found at a depth of ~1100 m in the Palmahim Disturbance within the Levantine Basin of the southeastern Mediterranean Sea (Herut et al. 2022, Rubin-Blum et al. 2024). This basin is one of the most oligotrophic marine environments, with low photosynthetically derived primary production and therefore very low inputs of organic nutrients into the deep hydrosphere (Hedges & Oades 1997, Herut et al. 2000, Krom et al. 2005). Seeps may contribute carbon and nitrogen to the deep-sea food webs in this basin, given the ^{13}C - and ^{15}N -depleted particulate organic matter (POM) ($\delta^{13}\text{C}_{\text{POM}} -27.3 \pm 0.5\text{‰}$ and $\delta^{15}\text{N}_{\text{POM}} 1.9 \pm 0.7\text{‰}$) near the Palmahim Disturbance seafloor (Sisma-Ventura et al. 2022). Palmahim Disturbance chemosynthetic communities resemble

those of other cold seeps in the deep eastern Mediterranean Sea (Olu-Le Roy et al. 2004, Carlier et al. 2010), and are inhabited by the vestimentiferan tubeworms *Lamellibrachia anaximandri*, bathymodioline mussels *Idas modiolaeformis*, and lucinid clams *Lucinoma kazani* (Zvi-Kedem et al. 2021, 2023, Ratinskaia et al. 2024), as well as by detritivores, such as *Clelandella myriamae* gastropods. The area surrounding the Palmahim Disturbance seeps is largely burrowed by ghost shrimps *Calliax lobata* (Basso et al. 2020, Rubin-Blum et al. 2025).

Most strikingly, the immediate surroundings of these pools serve as *G. melastomus* nurseries, with unprecedented egg densities (Herut et al. 2022, Sisma-Ventura et al. 2024). Large populations of the deepwater echinoid *Gracilechinus elegans* and the gastropod *C. myriamae* are associated with these breeding sites, suggesting a trophic link. To better understand the trophic ecology of Palmahim Disturbance cold seep fauna, we (1) assessed carbon sources and trophic position (TP) based on bulk stable carbon ($\delta^{13}\text{C}_{\text{bulk}}$) and nitrogen ($\delta^{15}\text{N}_{\text{bulk}}$) isotope values in tissues and (2) used compound-specific isotopic analysis of amino acids (CSIA-AA) to estimate TP independent of the confounding influence of trophic fractionation (McMahon et al. 2010). We further used CSIA-AA to determine the heterogeneity of nitrogen sources (Wang et al. 2022) and to predict the contribution of microbially reworked organics using microbial resynthesis (ΣV ; McCarthy et al. 2007, Vokhshoori et al. 2021, Suh et al. 2023) and leucine–isoleucine (Leu–Ile; Suh et al. 2023) indices.

2. MATERIALS AND METHODS

2.1. Study site and sampling

The Palmahim Disturbance is a deformation feature on the southeastern Mediterranean Sea margin, with hydrocarbon seeps at its toe, 65 km offshore from Israel (32° 10' N, 34° 10' E, water depth of approximately 1150 m). Samples were collected using a remotely operated vehicle (ROV 'Yona', SAAB Seaeeye Leopard) onboard the RV 'Bat Galim', on 2 successive expeditions conducted in April and November 2021 (Fig. 1). We collected specimens of the tubeworm *Lamellibrachia anaximandri* (5 individuals, different subsections of the plume, trophosome, and root; same specimens used for bulk and CSIA-AA analyses), bathymodioline mussel *Idas modiolaeformis* (1 and 5 distinct whole individuals for bulk and CSIA-AA anal-

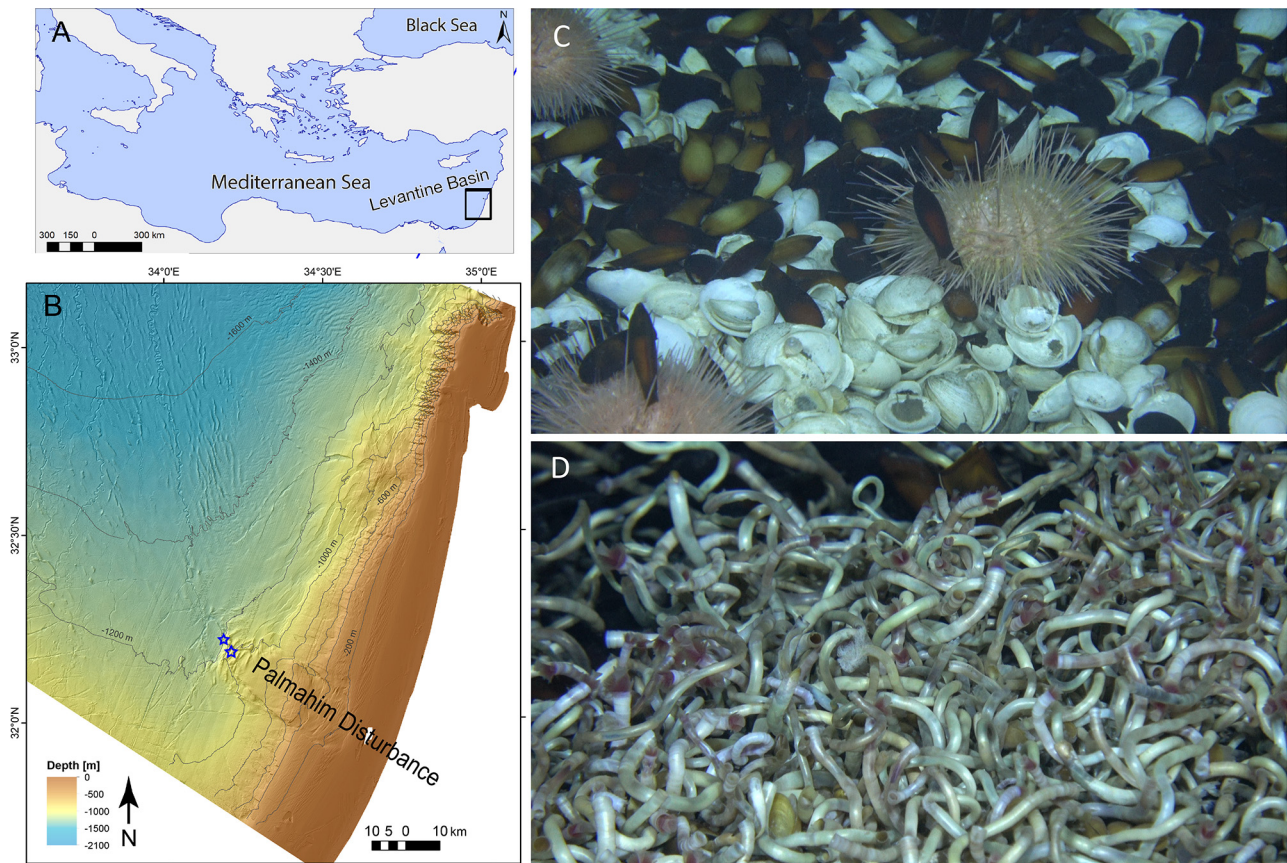


Fig. 1. (A,B) Sampling sites at the edge of the Palmahim Disturbance, eastern Mediterranean Sea: cold seeps at a water depth of 1150 m (blue stars in panel B mark the 2 collection sites). (C,D) *In situ* photographs of epibenthic communities at the site, as visualized by the remotely operated vehicle (ROV): (C) *Galeus melastomus* eggs accompanied by *Gracilechinus elegans* echinoids observed among *Lucinoma kazani* clams; (D) *G. melastomus* eggs within colonies of *Lamellibrachia anaximandri* tubeworms and *Idas modiolaeformis* mussels

yses, respectively), lucinid clam *Lucinoma kazani* (gill samples from 5 individuals, split for bulk and CSIA-AA analyses), ghost shrimp *Calliax lobata* (undefined tissues from 4 specimens used for bulk ($n = 4$) and CSIA-AA ($n = 3$) analyses), gastropod *Clelandella myriamae* (1 and 3 distinct whole individuals for bulk and CSIA-AA analyses, respectively), echinoid *Gracilechinus elegans* (undefined tissues from a single specimen for bulk; gonad, muscle, peristome, and undefined tissues for CSIA-AA analyses, 6 samples total), and blackmouth catshark *Galeus melastomus* eggs (3 eggs, divided into the embryo, yolk, and case, 8 and 7 samples for bulk and CSIA-AA analyses, respectively) (Tables S1 & S2 in Supplement 1 at www.int-res.com/articles/suppl/m756p071_supp/). The samples were preserved at -20°C until further analysis. The taxonomy was verified with genetics (metagenomics or Sanger sequencing of marker genes, data not shown for species where work is in progress; Zvi-Kedem et al. 2021, 2023).

2.2. Bulk stable isotope analysis

Bulk stable isotope analysis was performed on a total of 24 specimens. Samples were frozen and lyophilized for 24 h. Freeze-dried samples were homogenized and weighed before stable isotope analysis was conducted at the Cornell Stable Isotope Laboratory (Ithaca, NY, USA). The isotopic composition of organic carbon and nitrogen was determined by the analysis of CO_2 and N_2 continuous flow produced by combustion on a Carlo Erba NC2500 connected online to a DeltaV isotope ratio mass spectrometer coupled with a ConFlo III interface (Sisma-Ventura et al. 2022). Measured isotope ratios are reported in δ -notation and expressed relative to international standards of Vienna PeeDee belemnite (VPDB) and atmospheric N_2 for carbon and nitrogen, respectively. The analytical precision for the in-house standard was $\pm 0.04\text{‰}$ (1σ) for both $\delta^{13}\text{C}$ and $\delta^{15}\text{N}$ (Guy-Haim et al. 2022). Lipid correction was performed according to Post et

al. (2007). *C. myriamae* values were removed from the analysis due to aberrant C/N ratios (Table S1).

2.3. Compound-specific stable isotope analysis

Approximately 3 mg of lyophilized tissue were acid-hydrolyzed in 1 ml of 6 nmol HCl at 150°C for 75 min (Cowie & Hedges 1992) under a nitrogen atmosphere inside a 4 ml glass vial with a PTFE cap. Samples were cooled to room temperature (25°C) and HCl was then evaporated under a gentle stream of nitrogen. Samples were neutralized twice with 1 ml ultra-pure water and evaporation with a gentle stream of nitrogen. We used an EZ:faast (Phenomenex) amino acid analysis kit with a slight modification of replacing reagent 6 with dichloromethane as a solvent. For carbon analysis, we injected 1.5 μ l in split mode (1:15) and for nitrogen in splitless mode at 250°C. Helium was used as a carrier gas at a constant flow of 1.5 ml min⁻¹. The amino acids were separated on a Zebron ZB-50 column (30 m, 0.25 mm, and 0.25 μ m) in a Thermo Scientific Trace 1300 gas chromatograph (GC). The gas chromatography conditions were set to optimize peak separation for the desired amino acids as follows: initial temperature: 110°C, ramped to 240°C at 8°C min⁻¹ and then ramped to 320°C at 20°C min⁻¹ and held for 2.5 min. The separated amino acids were split on the MicroChannel Device into 2 direction flows, one toward the Thermo Scientific ISQ quadrupole for amino acid identification and the second toward the Thermo Scientific Delta V advantage for C and N isotope analysis. The ISQ condition was set to transfer line 310°C, ion source 240°C, and scan range from 43 to 450 *m/z* mass range. To define the isotopic ratio of carbon and nitrogen, separated amino acids were combusted in a Thermo Scientific GC Isolink II at 1000°C for CO₂ and N₂. Before entering the Delta V for the N₂ analysis, the sample went through a liquid nitrogen cold trap to freeze down all other gases. From each sample, duplicates were injected for carbon and triplicates for nitrogen.

2.4. Data analysis and corrections

We used CSIA-AA to determine isotopic fractionation values of carbon in essential or non-essential amino acids, and nitrogen in trophic or source amino acids (Whiteman et al. 2019). Essential amino acids (e.g. valine [Val], leucine [Leu], isoleucine [Ile], methionine [Met], and phenylalanine [Phe]) and source amino acids (e.g. Met, Phe, and glycine [Gly])

are unaffected during the transfer between trophic levels. In contrast, non-essential amino acids (e.g. aspartic acid [Asp], glutamic acid [Glu], proline [Pro], and alanine [Ala]) and trophic amino acids (e.g. Ile, Leu, Val, Asp, Ala, and Glu) differ between trophic levels (McClelland & Montoya 2002). Stable isotope ratios were expressed in standard δ notation relative to VPDB for carbon and atmospheric N₂ (air) for nitrogen. We used a standard that contains 7 amino acids of known isotopic ratio (Ala, Val, Leu, Ile, Met, Glu, and Phe) with an isotopic range for nitrogen of -6.69 to +43.25‰. Amino acids (Sigma Aldrich) were analyzed at the Geological Survey of Israel by elemental analyzer isotope ratio mass spectrometry, in addition to certified amino acids (Ala +43.25‰ and Val +30.19‰, Arndt Schimmelmann, Biogeochemical Laboratories, Indiana University, Bloomington, IN, USA). Since nitrogen was not added during derivatization, corrections for nitrogen addition were not required. To account for carbon that is incorporated during the derivatization process, a correction factor for each amino acid using the equation $n_{cd}\delta^{13}C_{cd} = n_c\delta^{13}C_c + n_d\delta^{13}C_{dcorr}$ where *n* is the number of moles of carbon, *C_c* is the compound of interest (amino acid), *C_{cd}* is the derivatized compound, and *C_{dcorr}* is the empirically determined correction factor (Docherty et al. 2001). The standard amino acid was used to set *C_{dcorr}* for later calculation of the isotopic ratio of our sample. The standard of amino acids was injected 3 times after the combustion reactor oxidation for carbon and 3 more times for nitrogen. To allow for drift correction, the standard was injected again 3 times for carbon and nitrogen after a maximum of 18 injections. Since amino acids differ in the presence of heteroatoms and functional groups, which may lead to different combustion efficiencies and therefore differences in drift, an average of the standard injection from the beginning and the end of the sequence was used. For each sequence of nitrogen, a correction factor was applied based on the linear regression equation of the ratio between the known amino acid isotopic ratio and the acquired result for the sequence. We note that derivatization protocols affect parameters of TP calculation, including β (the difference between the $\delta^{15}N$ values of Glu and Phe in primary producers) and TDF_{AA} (amino acid-specific trophic discrimination factor; McMahon & McCarthy 2016, Martinez et al. 2020). Thus, TP was calculated from the equation $TP_{Glu-Phe} = [(\delta^{15}N_{Glu} - \delta^{15}N_{Phe} - \beta)/TDF_{AA}] + 1$ where $\beta = -0.36$ and TDF_{AA} = 4.54 (Martinez et al. 2020), and using a range of β and TDF_{AA} determined previously (Chikaraishi et al. 2009, Nielsen et al. 2015, Martinez et al. 2020).

To test differences in TP among species, we used the Kruskal–Wallis test and Dunn’s post hoc multiple comparisons (excluding species with fewer than 5 specimens), in R version 3.3.6 (R Core Team 2024). Differences were considered significant at $p < 0.05$. Graphs were generated using the R package ‘ggplot2’ (Wickham 2016) and SigmaPlot V14.0 (Systat Software).

3. RESULTS

3.1. Bulk $\delta^{13}\text{C}$ and $\delta^{15}\text{N}$ values of macrofauna

We observed a wide range of bulk carbon isotope values ($\delta^{13}\text{C}_{\text{bulk}}$) in the tissues of Palmahim Disturbance fauna (Fig. 2, Table 1; Table S1). The mussel *Idas modiolaeformis* had the lowest $\delta^{13}\text{C}_{\text{bulk}}$ of -58.0‰ , whereas $\delta^{13}\text{C}_{\text{bulk}}$ values were -40.7 ± 2.7 and $-30.8 \pm 0.8\text{‰}$ in tissues of the symbiont-bearing vestimentiferan tubeworm *Lamellibrachia anaximandri* and the lucinid clam *Lucinoma kazani*, respectively. In *Galeus*

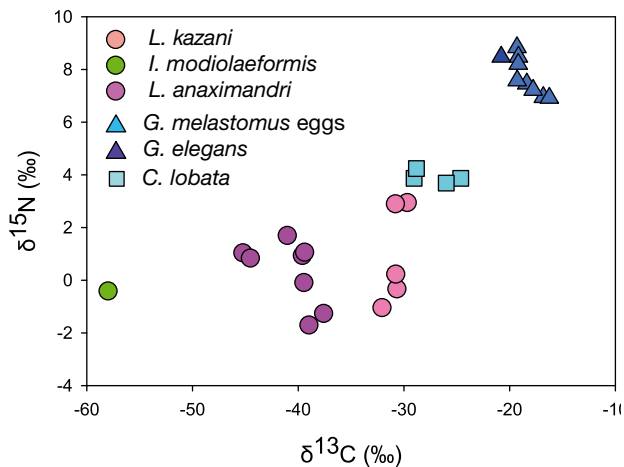


Fig. 2. Carbon and nitrogen stable isotope ratios (‰) in symbiont-bearing and heterotrophic fauna, collected at Palmahim Disturbance cold seeps

melastomus eggs, $\delta^{13}\text{C}_{\text{bulk}} = -18.3 \pm 1.2\text{‰}$ was similar to values of $-17.8 \pm 0.3\text{‰}$ measured in adults (Guy-Haim et al. 2022). In the putative detritivore *Gracilechinus elegans*, $\delta^{13}\text{C}_{\text{bulk}}$ was -20.8‰ , and *Calliax lobata* $\delta^{13}\text{C}_{\text{bulk}}$ was $-27.1 \pm 2.2\text{‰}$. Lipid correction often resulted in minor shifts in $\delta^{13}\text{C}_{\text{bulk}}$ values, except in several specimens with high C/N ratios, e.g. *G. elegans* (C/N ratio = 8.5, $\delta^{13}\text{C}_{\text{bulk_corrected}} = -15.7\text{‰}$) and *L. kazani* (C/N ratio = 9.2, $\delta^{13}\text{C}_{\text{bulk_corrected}} = -23.9\text{‰}$) (Table S1).

We observed a wide range of $\delta^{15}\text{N}$ values, from -1.7 to 8.8‰ . In chemosynthetic fauna, we often detected the lowest $\delta^{15}\text{N}$, for example, minimum values of -1.7‰ in *L. anaximandri*, -1.0‰ in *L. kazani* and -0.4‰ in *I. modiolaeformis* (Table 1). *C. lobata* had intermediate $\delta^{15}\text{N}$ values of 4.75 ± 0.2 . The $\delta^{15}\text{N}$ in *G. melastomus* eggs ($7.7 \pm 0.7\text{‰}$) reflected $\delta^{15}\text{N} = 7.9 \pm 0.1\text{‰}$ determined previously in adults from the Levantine basin (Guy-Haim et al. 2022). $\delta^{15}\text{N}$ was 8.5‰ in a single *G. elegans* specimen.

3.2. Compound-specific amino acid isotopes

To further evaluate the differences in carbon and nitrogen sources of all sampled species, we examined the $\delta^{13}\text{C}$ and $\delta^{15}\text{N}$ values of each amino acid individually. Following bulk analyses, *I. modiolaeformis* ($n = 5$) exhibited the lowest $\delta^{13}\text{C}$ values (down to -73.6‰ for Val), whereas the embryos of *G. melastomus* and *G. elegans* exhibited higher values ($\delta^{13}\text{C}_{\text{Val}} = -22.8 \pm 3.8\text{‰}$ and $-25.5 \pm 4.8\text{‰}$, respectively; Fig. 3; Table S2). The $\delta^{13}\text{C}$ values were lower, yet variable in *L. anaximandri*, which displayed a large variation in carbon sources (e.g. $\delta^{13}\text{C}_{\text{Val}}$ between -44.9 and -60.2‰). The non-symbiotic *Clelandella myriamae* had similar values ($\delta^{13}\text{C}_{\text{AA}} = -45.7 \pm 5.4\text{‰}$; Fig. 3; Table S2), in line with previous estimates of $\delta^{13}\text{C}_{\text{bulk}}$ ($-35.2 \pm 3.5\text{‰}$) in *C. myriamae* from the Amsterdam mud volcano (Carlier et al. 2010). *C. lobata* showed

Table 1. Bulk $\delta^{13}\text{C}$ and $\delta^{15}\text{N}$ values (mean \pm SD, max, min) of macrofauna collected from the Palmahim Disturbance cold seeps (see Table S1 in Supplement 2 for detailed information). VPDB: Vienna PeeDee belemnite

Species	n	Group	$\delta^{13}\text{C}$ (‰ vs. VPDB)			$\delta^{15}\text{N}$ (‰ vs. air)		
			Mean	Max.	Min.	Mean	Max.	Min.
<i>Lucinoma kazani</i>	5	Bivalves	-30.8 ± 0.8	-29.7	-32.1	0.9 ± 1.8	2.9	-1.0
<i>Idas modiolaeformis</i>	1	Bivalves	-58.0	-58.0	-58.0	-0.4	-0.4	-0.4
<i>Lamellibrachia anaximandri</i>	5	Siboglinids	-40.7 ± 2.7	-37.6	-45.2	0.3 ± 1.2	1.7	-1.7
<i>Gracilechinus elegans</i>	1	Echinoderms	-20.8	-20.8	-20.8	8.5	8.5	8.5
<i>Galeus melastomus</i>	7	Elasmobranchs	-18.3 ± 1.2	-16.3	-19.3	7.7 ± 0.7	8.8	6.9
<i>Calliax lobata</i>	3	Crustaceans	-27.1 ± 2.1	-29.0	-24.6	4.8 ± 0.2	4.2	3.7

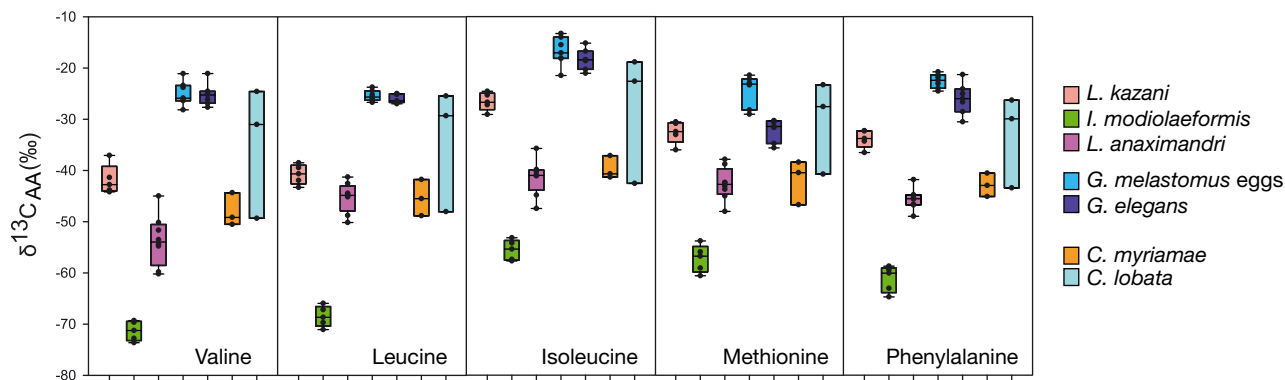


Fig. 3. Carbon stable isotope ratios ($\delta^{13}\text{C}_{\text{AA}}$, ‰) in each of 5 essential amino acids (valine, leucine, isoleucine, methionine, and phenylalanine) of symbiont-bearing and heterotrophic fauna from Palmahim Disturbance seeps (compound-specific isotopic analysis of amino acids, CSIA-AA). The horizontal line represents the median value of the data set; boxes show the interquartile range, spanning the 25th to the 75th percentile; whiskers extend to the maximum and minimum data values, circles show the values in the data set. See Table S2 in Supplement 2 for detailed information

the highest variation in $\delta^{13}\text{C}_{\text{AA}}$ values ($-32.2 \pm 9.9\text{‰}$, $n = 3$).

The source amino acids Gly, Met, and Phe were consistently depleted in ^{15}N compared to the trophic amino acids Ala, Val, Leu, Ile, Asp, and Glu (Fig. 4; Table S2). *L. anaximandri*, *L. kazani*, and *Idas* sp. consistently displayed the most negative $\delta^{15}\text{N}$ values. Glycine was depleted in ^{15}N relative to other amino acids, with the amino acid value of the clam *L. kazani* the most ^{15}N depleted ($\delta^{15}\text{N} = -13.3 \pm 1.7\text{‰}$; Fig. 4; Table S2). Amino acids of the putative top consumers *G. elegans* and *G. melastomus* were enriched in ^{15}N , compared to others. *C. myriamae* and *C. lobata* had intermediate $\delta^{15}\text{N}$ values. For example, Leu $\delta^{15}\text{N}$ values of *C. myriamae* (13.0‰) and *C. lobata* (12.6‰) were lower than those of *G. elegans* (21.8‰) and higher than those of *L. anaximandri* (-1.93‰) (Fig. 4; Table S2).

Differences in $\delta^{15}\text{N}$ and $\delta^{13}\text{C}$ values between species within each amino acid were evaluated using the Kruskal-Wallis test (Kruskal-Wallis chi-squared = 15.7, $df = 4$, $p = 0.003$). Pairs that were found to be significantly different according to the post hoc Dunn's

test were *I. modiolaeformis* – *G. elegans*, *I. modiolaeformis* – *G. melastomus*, *G. elegans* – *L. anaximandri*, and *G. melastomus* – *L. anaximandri* for all $\delta^{13}\text{C}_{\text{AA}}$ (adjusted $p < 0.05$) (Table S3). Similar results were obtained for $\delta^{15}\text{N}_{\text{AA}}$, except for the amino acid glycine where all species differences were statistically insignificant except for *L. kazani* – *G. elegans* (adjusted $p = 0.0001$) (Table S3). Plotting the C versus N stable isotope values from essential amino acids suggests that nutrition sources differed for the studied biota, with clustering of *G. melastomus* and *G. elegans* and a clear separation of carbon values in chemosynthetic fauna, including *L. anaximandri*, *I. modiolaeformis*, and *L. kazani* (Fig. 5). These values in *C. myriamae* did not cluster with either of the groups, while *C. lobata* data were noisy, with no clear clustering pattern.

3.3. Microbial resynthesis index and AA-CSIA-based TP

To evaluate the extent of heterotrophy in symbiont-bearing and other taxa, we employed microbial resyn-

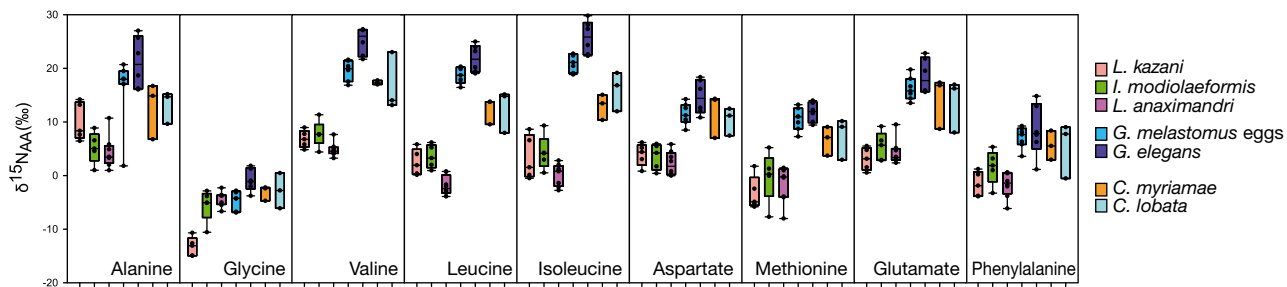


Fig. 4. Nitrogen stable isotope ratios ($\delta^{15}\text{N}_{\text{AA}}$, ‰) in trophic amino acids of symbiont-bearing and heterotrophic fauna from Palmahim Disturbance seeps (CSIA-AA). Boxplot parameters as in Fig. 3

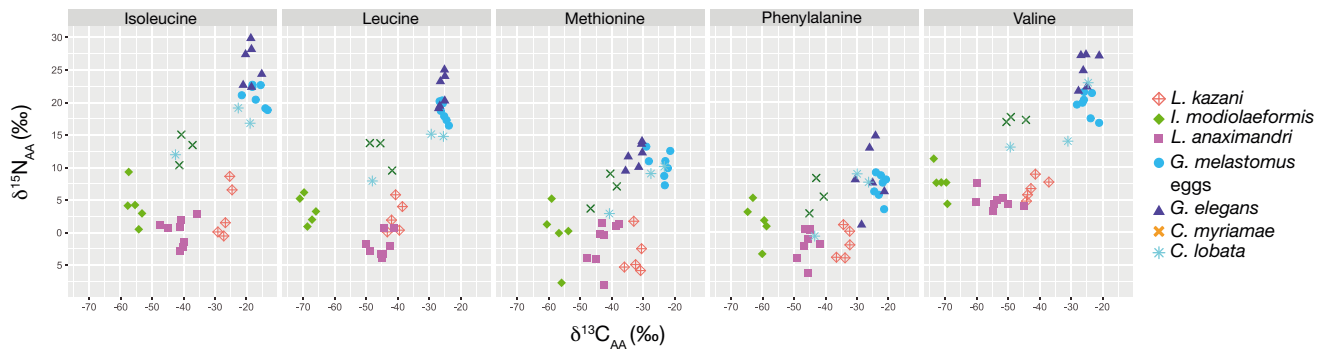


Fig. 5. Carbon stable isotope ratios ($\delta^{13}\text{C}_{\text{AA}}$, ‰) and nitrogen stable isotope ratios ($\delta^{15}\text{N}_{\text{AA}}$, ‰) in amino acids (CSIA-AA) of symbiont-bearing and heterotrophic fauna from Palmahim Disturbance seeps, shown as biplots. See Table S2 in Supplement 2 for detailed information

thesis (ΣV) (McCarthy et al. 2007) and Leu–Ile (Suh et al. 2023) indices. We note that $\delta^{15}\text{N}$ in Pro was not estimated, so the calculation of the ΣV and Leu–Ile indices in our study deviates from that reported previously. Yet, even disregarding the Pro value, the Leu–Ile index indicated a clear separation between chemosynthetic and heterotrophic fauna, where the highest values were detected in *L. anaximandri* (5.4 ± 1.3 ; Fig. 6A). Among the chemosynthetic fauna, we identified the largest variation in the Leu–Ile index in *I. modiolaeformis* (2.2 ± 1.3), with the lowest value reaching -0.8 (Fig. 6A). In *L. kazani*, the Leu–Ile index was 3.8 ± 1.1 . This is opposed to usually negative values in *G. melastomus* and *G. elegans* (Fig. 6A). Very noisy Leu–Ile index values were found in *C. lobata* (0.2 ± 2.0) and *C. myriamae* (2.1 ± 2.5). ΣV values correlated well with the Leu–Ile index (Fig. 6B). We observed a positive correlation ($\Sigma\text{V} = 0.3(\text{Leu} - \text{Ile}) + 1.0$, $r^2 = 0.7$) for symbiont-bearing taxa, and negative for heterotrophic species ($\Sigma\text{V} = -0.5(\text{Leu} - \text{Ile}) + 1.1$, $r^2 = 0.7$).

To estimate the TP of the seep biota, we calculated nitrogen AA-CSIA (Glu–Phe), using $\beta = -0.36$ and $\text{TDF}_{\text{AA}} = 4.54$ (Martinez et al. 2020), given that the use of respective derivatization protocol. We also calculated TPs using a range of β and TDF_{AA} determined previously (Chikaraishi et al. 2009, Nielsen et al. 2015, Martinez et al. 2020), often resulting in lower TPs across the whole data set (Fig. S1 in Supplement 2 at www.int-res.com/articles/suppl/m756p071_supp/, Table S2). We estimated the lowest TP in chemosynthetic taxa, including *I. modiolaeformis* ($\text{TP} = 1.9 \pm 0.6$) and *L. kazani* (2.1 ± 0.1) (Fig. 6C). A broader TP range was found in *L. anaximandri* (2.4 ± 0.7). The highest TP was observed among *G. elegans* (3.4 ± 0.9), exceeding that of *G. melastomus* embryos (3.2 ± 0.4). Intermediate, yet noisy TP

characterized *C. myriamae* (3.1 ± 1.2) and *C. lobata* (3.0 ± 0.1). We found a poor interdependence of TP and Leu–Ile index (Fig. 6D).

4. DISCUSSION

Palmahim Disturbance seeps accumulate unprecedented numbers of *Galeus melastomus* eggs and their cases. The massive shark nursery appears to introduce an unexpected nutrition source, as *G. melastomus* eggs may integrate into the Palmahim Disturbance food web. The presence of *G. melastomus* eggs was often linked to the occurrence of detritivores such as *Clelandella myriamae*, and most importantly, *Gracilechinus elegans* echinoderms, which were found in large numbers only in the shark nursery. The high similarity of bulk carbon and nitrogen stable isotopes in *G. elegans* and *G. melastomus*, as well as the fact that the highest $\text{TP}_{(\text{Glu}-\text{Phe})}$ in our data set was found in a *G. elegans* specimen (4.7 ; Fig. 5), suggest that these echinoderms may feed on shark eggs (shared resources are unlikely). This is further supported by the fact that most *G. elegans* were associated with the shark nursery, and our observation of a *G. elegans* specimen feeding on *G. melastomus* egg *ex situ* upon sample retrieval. However, a chemosynthetic component may be present in *G. elegans* diet, given the slight shift towards lower $\delta^{13}\text{C}_{\text{AA}}$ values, a fluctuating $\text{TP}_{(\text{Glu}-\text{Phe})}$, and a resynthesis index often higher than that of *G. melastomus* eggs (Fig. 6). This reflects the fact that echinoids frequently engage in opportunistic feeding on detritus, but can also be predators, hence feeding at different trophic levels (Durden et al. 2020). In particular, cold-water corals comprised a substantial fraction of *G. elegans* diet in the NE Atlantic deep-sea submarine

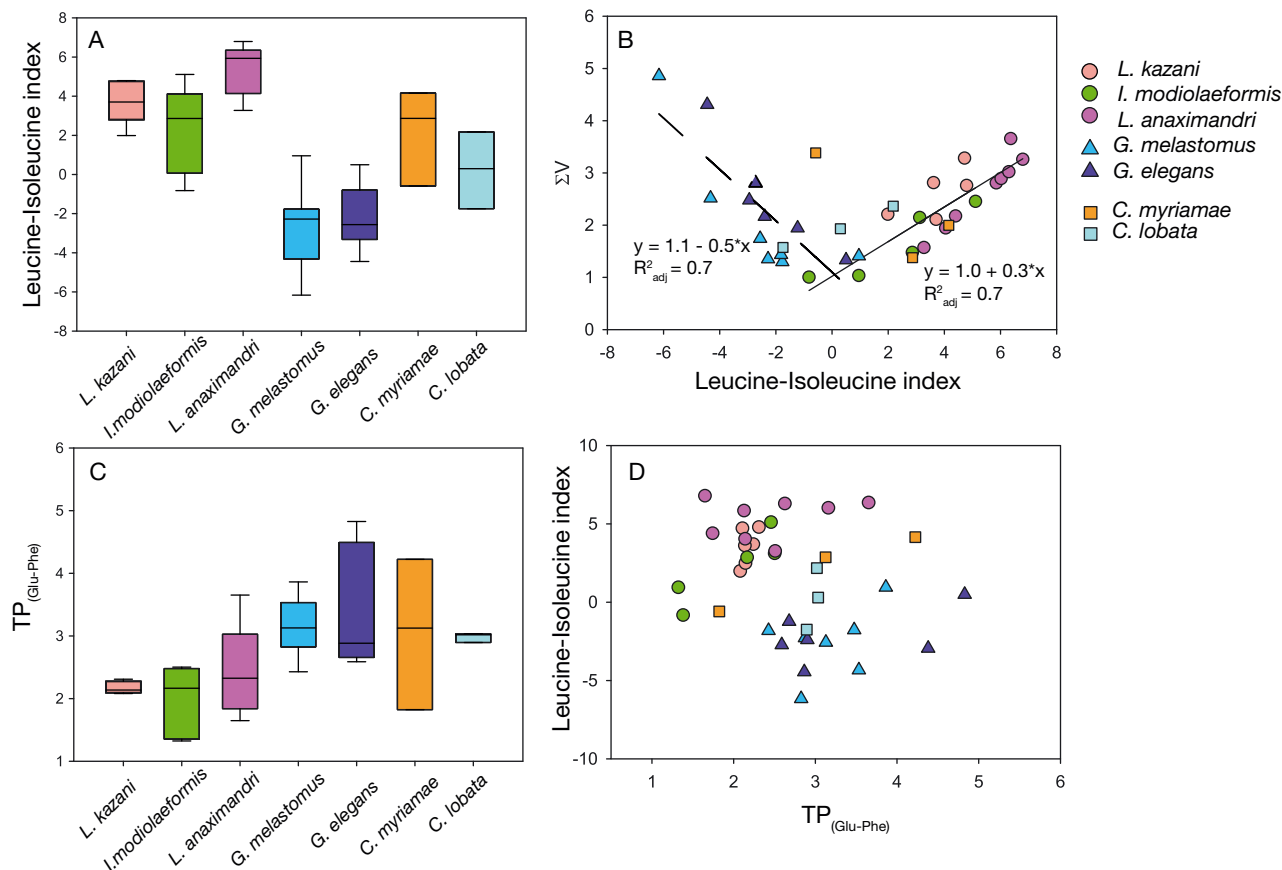


Fig. 6. Microbial resynthesis index (ΣV) and CSIA-AA-based trophic positions in Palmahim Disturbance seep fauna. (A) Leucine–isoleucine index. (B) ΣV as a function of the leucine–isoleucine index. (C) Trophic position (TP) as determined by CSIA-AA (glutamic-acid–phenylalanine, Glu–Phe) using $\beta = -0.36$ and amino acid-specific trophic discrimination factor ($TDF_{AA} = 4.54$ (Martinez et al. 2020)). The horizontal line represents the median value of the data set; boxes show the interquartile range, spanning the 25th to the 75th percentile; whiskers extend from the box to the maximum and minimum data values. (D) Leucine–isoleucine index as a function of TP

canyons (Stevenson & Mitchell 2016). Our findings suggest that their nutrition surprisingly extends to *G. melastomus* egg cases.

Our data indicates that apart from these unusual inputs, the Palmahim Disturbance cold seep fauna is largely supported by chemosynthetic productivity. This is evidenced by the fact that the majority of $\delta^{13}C$ values are lower than the typical bulk $\delta^{13}C$ -14 to -20‰ found in non-seep benthic consumers that exclusively feed on sinking photosynthesized organic material (Carlier et al. 2010, Toone & Washburn 2020, Guy-Haim et al. 2022). The negative bulk $\delta^{15}N$ values between -1.04 and -1.69‰ in chemosynthetic fauna indicate that the symbionts use local nitrogen sources (Vokhshoori et al. 2021). Following previous work (Carlier et al. 2010), and current knowledge of symbioses at Palmahim Disturbance seeps, bulk $\delta^{13}C$ values between -32.1 and -58.0‰ reflect the variation in dependence on methane-derived car-

bon in chemosynthetic taxa (in nearby sediments $\delta^{13}C_{CH_4}$ was circa -62‰ ; B. Herut pers. comm.). These taxa include *Idas modiolaeformis*, whose main symbionts use methane as a carbon source (Duperron et al. 2008, Duperron 2010, Zvi-Kedem et al. 2023), to *Lamellibrachia anaximandri* and *Lucinoma kazani*, whose symbionts mainly fix inorganic carbon (Zvi-Kedem et al. 2021, Ratinskaia et al. 2024). We note that lipid correction due to elevated C/N ratio in some individuals resulted in higher $\delta^{13}C_{bulk}$ (circa 2‰ shifts for chemosynthetic fauna), and a larger variation among individuals (e.g. $-28.3 \pm 2.6\text{‰}$ lipid corrected, as opposed to $-30.8 \pm 0.8\text{‰}$ in uncorrected $\delta^{13}C_{bulk}$ of *L. kazani*; Table S1). Despite these uncertainties in $\delta^{13}C_{bulk}$ values, the chemosynthetic origin of carbon in these species is evident.

We show evidence for spatial variation in the contribution of methane-derived carbon to the DIC pool, which is likely linked to fluxes, and consequently, to

specific ecological niches occupied by different fauna. For example, *L. anaximandri* and *L. kazani*, both hosting sulfur-oxidizing symbionts, aggregated in distinct zones, and rarely co-occurred (Video S1 at www.int-res.com/articles/suppl/m756p071_supp/). In turn, we observed a circa 10‰ shift in bulk $\delta^{13}\text{C}$ between *L. anaximandri* and *L. kazani*, hinting that methane-derived DIC is an important source of carbon for *L. anaximandri*, given that no methane-oxidizing symbionts were found in these hosts (Zvi-Kedem et al. 2021, Ratinskaia et al. 2024). While we identified similar shifts in $\delta^{13}\text{C}$ in most essential amino acids, the differences in Leu $\delta^{13}\text{C}$ values were negligible for *L. kazani* and *L. anaximandri*. This phenomenon may be linked to the fact that *L. anaximandri* symbionts fix carbon using not only the Calvin-Benson-Bassham cycle but also the reverse tricarboxylic cycle, which enriches its products in ^{13}C (van der Meer et al. 1998) and yields the leucine precursor pyruvate (Rubin-Blum et al. 2019, Zvi-Kedem et al. 2021).

The $\text{TP}_{(\text{Glu}-\text{Phe})}$ estimates reflect the heterogeneity of nutrient assimilation strategies and sources in the Palmahim Disturbance seep fauna. Aberrant TPs were estimated previously in trophosomes of the tubeworm *Lamellibrachia columna* ($\text{TP} = 2.6 \pm 0.1$, higher than those expected for an animal whose nutrition relies solely on the chemosynthetic symbionts), hypothetically due to complex nutritional interactions between the symbiont and the host (Ishikawa et al. 2024). We observed a similar pattern of high and heterogeneous TP values in *L. anaximandri* ($\text{TP}_{(\text{Glu}-\text{Phe})} = 2.4 \pm 0.7$; Fig. 6C). *Lucinoma kazani* and *I. modiolaeformis* ($\text{TP}_{(\text{Glu}-\text{Phe})}$ (2.1 ± 0.1 and 1.9 ± 0.6 , respectively; Fig. 6C) followed previous estimates in other basins, for example, $\text{TP} = 2.3 \pm 0.2$ and 1.8 ± 0.2 in the vent mussels *Bathymodiolus septemdierum* and *Gigantidas vrijenhoeki*, respectively (Suh et al. 2023), and the maximum TP was estimated at 2.2 ± 0.5 in *B. childressi* from the NE Atlantic Margin (Vokhshoori et al. 2021).

Substantial fluctuations in the *I. modiolaeformis* resynthesis index suggest that its nitrogen may derive not only from assimilation by chemosynthetic bacteria but also from alternative sources. Chemosynthetic mollusks can feed on photosynthetically derived or suspended sedimentary POM (Vokhshoori et al. 2021, Peketi et al. 2022), using organic rather than inorganic nitrogen sources (Wang et al. 2022). It is unknown if the small *Idas* mussels can feed on POM directly. In turn, *I. modiolaeformis* harbors a larger diversity of symbionts than most bathymodioline mussels, enabling it to thrive on organic substrates, such as woodfalls (Olu-Le Roy et al. 2004, Duperron

et al. 2008, Zvi-Kedem et al. 2023). In the case of the Palmahim Disturbance seeps, organic substrates for the heterotrophic symbionts may include shark egg-derived compounds, such as collagen (Zvi-Kedem et al. 2023). Our *in situ* observations of *I. modiolaeformis* feeding on shark eggs support this hypothesis (Video S1). Alternatively, anaerobic breakdown of the shark eggs may release reduced compounds such as sulfide, fuelling chemosynthetic symbionts.

The putative detritivores *C. myriamae* and *C. lobata* occupy distinct niches in the Palmahim Disturbance seeps. *C. myriamae* was observed in large numbers in various niches, including the shark nursery, *L. anaximandri* reefs, and authigenic carbonates (Video S1). In turn, the diet of *C. myriamae* often depends on chemosynthetic bacteria, given the light $\delta^{13}\text{C}_{\text{AA}}$ of $-45.7 \pm 5.4\%$. These values are in line with $\delta^{13}\text{C}_{\text{bulk}}$ of $-35.2 \pm 3.5\%$ in *C. myriamae* from the Amsterdam mud volcano (Carlier et al. 2010). The resynthesis indices and TP markedly varied among *C. myriamae* specimens (minimum Leu–Iso index = -0.6 and $\text{TP} = 1.7$, maximum Leu–Iso index = 4.2 and $\text{TP} = 4.1$), suggesting opportunistic nutrition, which is likely to include decomposing shark eggs. *C. lobata* do not occur in the shark nursery, but occupy the seep periphery (chemotone, Ashford et al. 2021) and may employ a gardening-like feeding strategy (Rubin-Blum et al. 2025). Subsequently, we found consistent $\delta^{13}\text{C}$ values and TP in *C. lobata* ($\delta^{13}\text{C}_{\text{bulk}}$ of $-27.1 \pm 2.2\%$, $\delta^{13}\text{C}_{\text{AA}}$ of $-32.2 \pm 9.9\%$, $\text{TP} = 2.9 \pm 0.1$), but the Leu–Iso index (minimum -1.7 and maximum 2.2) was surprisingly variable. For both *C. myriamae* and *C. lobata*, a larger sampling effort is needed to validate our estimates.

5. CONCLUSIONS

Food webs in seep and vent habitats largely rely on chemosynthetic productivity, while external inputs are usually small and depend on the downward flux of the chemosynthetically derived POM. These fluxes are particularly low in oligotrophic basins such as the eastern Mediterranean Sea, where autochthonous inputs likely predominate. Substantial heterogeneity of carbon and nitrogen sources, often in closely related animals that co-occur, complicates our understanding of trophic ecology in these habitats, where nutritional symbioses with microbes are crucial. This study exemplifies how CSIA-AA provides an important addition to bulk stable isotope analyses, not only estimating TP but also providing insights into microbial synthesis/resynthesis of key nutrition components.

In Palmahim Disturbance seeps, *Galeus melastomus* eggs and their cases appear to introduce an unexpected and massive source of nutrition to the seep habitat. Such aggregations were previously observed in nearby Nile Deep Sea Fan mud volcano at lower densities by Treude et al. (2011), indicating that this phenomenon is widespread in this basin. Yet, its extent remains to be quantified. *G. melastomus* nurseries are associated not only with seeps but also with cold-water coral habitats in the Atlantic Ocean (Henry et al. 2013), complementing the food webs in these vulnerable and essential habitats. The biopolymer-rich shark egg cases may enter the food web not only via direct consumption, but also by microbial decomposition, becoming the source of nutrition for detritivores, as well as unexpected consumers such as bathymodioline *Idas* mussels, likely adding unknown hubs for population connectivity. Microbial degradation of natural polymers may boost productivity, as in the case of giant sponge grounds at Arctic seamounts (Morganti et al. 2022). This phenomenon remains to be explored.

Acknowledgements. We thank all individuals who helped during the expeditions, including onboard technical and scientific personnel, the captain and crew of the IOLR RV 'Bat Galim', and the University of Haifa team operating ROV 'Yona'. This study was supported by the Horizon Europe project REDRESS (Restoration of deep-sea habitats to rebuild European Seas; Grant Agreement 101135492) to M.R.B. and Y.M., the Israeli Science Foundation (ISF) grants 913/19 and 1359/23 to M.R.B., Israel Ministry of Energy grants 221-17-002 (Y.M.) and 221-17-004 (M.R.B.) and the Mediterranean Sea Research Center of Israel (MERC I). This work was partly supported by the National Monitoring Program of Israel's Mediterranean waters and the Charney School of Marine Sciences (CSMS), University of Haifa.

LITERATURE CITED

- Ashford OS, Guan S, Capone D, Rigney K and others (2021) A chemosynthetic ecotone — 'chemotone' — in the sediments surrounding deep-sea methane seeps. *Limnol Oceanogr* 66:1687–1702
- Åström EKL, Carroll ML, Sen A, Niemann H, Ambrose WG Jr, Lehmann MF, Carroll JL (2019) Chemosynthesis influences food web and community structure in high-Arctic benthos. *Mar Ecol Prog Ser* 629:19–42
- Åström EKL, Bluhm BA, Rasmussen TL (2022) Chemosynthetic and photosynthetic trophic support from cold seeps in Arctic benthic communities. *Front Mar Sci* 9: 910558
- Carlier A, Ritt B, Rodrigues C, Sarrazin J (2010) Heterogeneous energetic pathways and carbon sources on deep eastern Mediterranean cold seep communities. *Mar Biol* 157:2545–2565
- Chikaraishi Y, Ogawa NO, Kashiyama Y, Takano Y and others (2009) Determination of aquatic food-web structure based on compound-specific nitrogen isotopic composition of amino acids. *Limnol Oceanogr Methods* 7:740–750
- Cordes EE, Becker EL, Fisher CR (2010) Temporal shift in nutrient input to cold-seep food webs revealed by stable-isotope signatures of associated webs communities. *Limnol Oceanogr* 55:2537–2548
- Cowie GL, Hedges JI (1992) Improved amino acid quantification in environmental samples: charge-matched recovery standards and reduced analysis time. *Mar Chem* 37: 223–238
- Docherty G, Jones V, Evershed RP (2001) Practical and theoretical considerations in the gas chromatography/com-bustion/isotope ratio mass spectrometry $\delta^{13}\text{C}$ analysis of small polyfunctional compounds. *Rapid Commun Mass Spectrom* 15:730–738
- Duperron S (2010) The diversity of deep-sea mussels and their bacterial symbioses. In: Kiel S (ed) *The vent and seep biota*. Topics in Geobiology 33. Springer Netherlands, Dordrecht, p 137–167
- Duperron S, Halary S, Lorion J, Sibuet M, Gaill F (2008) Unexpected co-occurrence of six bacterial symbionts in the gills of the cold seep mussel *Idas* sp. (Bivalvia: Mytilidae). *Environ Microbiol* 10:433–445
- Durden JM, Bett BJ, Huffard CL, Pebody C, Ruhl HA, Smith KL (2020) Response of deep-sea deposit-feeders to detrital inputs: a comparison of two abyssal time-series sites. *Deep Sea Res II* 173:104677
- Guy-Haim T, Stern N, Sisma-Ventura G (2022) Trophic ecology of deep-sea megafauna in the ultra-oligotrophic southeastern Mediterranean Sea. *Front Mar Sci* 9:857179
- Hedges J, Oades J (1997) Comparative organic geochemistries of soils and marine sediments. *Org Geochem* 27: 319–361
- Henry LA, Navas JM, Hennige SJ, Wicks LC, Vad J, Murray Roberts J (2013) Cold-water coral reef habitats benefit recreationally valuable sharks. *Biol Conserv* 161:67–70
- Herut B, Almogi-Labin A, Jannik N, Gertman I (2000) The seasonal dynamics of nutrient and chlorophyll *a* concentrations on the SE Mediterranean shelf-slope. *Oceanol Acta* 23:771–782
- Herut B, Rubin-Blum M, Sisma-Ventura G, Jacobson Y and others (2022) Discovery and chemical composition of the eastmost deep-sea anoxic brine pools in the Eastern Mediterranean Sea. *Front Mar Sci* 9:1040681
- Ishikawa NF, Chen C, Hashimoto R, Ogawa NO, Uyeno D, Nomaki H (2024) Amino acid nitrogen isotopic compositions show seep copepods gain nutrition from host animals. *Mar Ecol Prog Ser* 727:81–90
- Jørgensen BB, Boetius A (2007) Feast and famine — microbial life in the deep-sea bed. *Nat Rev Microbiol* 5:770–781
- Joye SB (2020) The geology and biogeochemistry of hydrocarbon seeps. *Annu Rev Earth Planet Sci* 48:205–231
- Krom MD, Woodward EMS, Herut B, Kress N and others (2005) Nutrient cycling in the south east Levantine basin of the eastern Mediterranean: results from a phosphorus starved system. *Deep Sea Res II* 52:2879–2896
- Levin LA (2005) Ecology of cold seep sediments: interactions of fauna with flow, chemistry and microbes. *Oceanogr Mar Biol Annu Rev* 43:1–46
- MacAvoy SE, Carney RS, Fisher CR, Macko SA (2002) Use of chemosynthetic biomass by large, mobile, benthic predators in the Gulf of Mexico. *Mar Ecol Prog Ser* 225:65–78
- Martinez S, Lallar M, Shemesh E, Einbinder S, Goodman Tchernov B, Tchernov D (2020) Effect of different derivatization protocols on the calculation of trophic position

- using amino acids compound-specific stable isotopes. *Front Mar Sci* 7:561568
- ✦ McCarthy MD, Benner R, Lee C, Fogel ML (2007) Amino acid nitrogen isotopic fractionation patterns as indicators of heterotrophy in plankton, particulate, and dissolved organic matter. *Geochim Cosmochim Acta* 71:4727–4744
- ✦ McClelland JW, Montoya JP (2002) Trophic relationships and the nitrogen isotopic composition of amino acids in plankton. *Ecology* 83:2173–2180
- ✦ McMahon KW, McCarthy MD (2016) Embracing variability in amino acid $\delta^{15}\text{N}$ fractionation: mechanisms, implications, and applications for trophic ecology. *Ecosphere* 7:e01511
- ✦ McMahon KW, Fogel ML, Elsdon TS, Thorrold SR (2010) Carbon isotope fractionation of amino acids in fish muscle reflects biosynthesis and isotopic routing from dietary protein. *J Anim Ecol* 79:1132–1141
- ✦ Morganti TM, Slaby BM, de Kluijver A, Busch K and others (2022) Giant sponge grounds of Central Arctic seamounts are associated with extinct seep life. *Nat Commun* 13:638
- ✦ Nielsen JM, Popp BN, Winder M (2015) Meta-analysis of amino acid stable nitrogen isotope ratios for estimating trophic position in marine organisms. *Oecologia* 178:631–642
- ✦ Olu-Le Roy K, Sibuet M, Fiala-Médioni A, Gofas S and others (2004) Cold seep communities in the deep eastern Mediterranean Sea: composition, symbiosis and spatial distribution on mud volcanoes. *Deep Sea Res I* 51:1915–1936
- ✦ Olu K, Caprais JC, Galéron J, Causse R and others (2009) Influence of seep emission on the non-symbiont-bearing fauna and vagrant species at an active giant pockmark in the Gulf of Guinea (Congo-Angola margin). *Deep Sea Res II* 56:2380–2393
- ✦ Peketi A, Mazumdar A, Sawant B, Manaskanya A, Zatale A (2022) Biogeochemistry and trophic structure of a cold seep ecosystem, offshore Krishna-Godavari basin (east coast of India). *Mar Petrol Geol* 138:105542
- ✦ Pop Ristova P, Wenzhöfer F, Ramette A, Felden J, Boetius A (2015) Spatial scales of bacterial community diversity at cold seeps (Eastern Mediterranean Sea). *ISME J* 9:1306–1318
- ✦ Portail M, Olu K, Dubois SF, Escobar-Briones E, Gelinas Y, Menot L, Sarrazin J (2016) Food-web complexity in Guaymas Basin hydrothermal vents and cold seeps. *PLOS ONE* 11:e0162263
- ✦ Post DM, Layman CA, Arrington DA, Takimoto G, Quattrochi J, Montaña CG (2007) Getting to the fat of the matter: models, methods and assumptions for dealing with lipids in stable isotope analyses. *Oecologia* 152:179–189
- ✦ Ratinskaia L, Malavin S, Zvi-Kedem T, Vintila S, Kleiner M, Rubin-Blum M (2024) Metabolically-versatile *Ca. Thiodiazotropha* symbionts of the deep-sea lucinid clam *Lucinoma kazani* have the genetic potential to fix nitrogen. *ISME Commun* 4:ycae076
- ✦ Core Team (2024) R: a language and environment for statistical computing. R Foundation for Statistical Computing, Vienna
- ✦ Rubin-Blum M, Antony CP, Sayavedra L, Martínez-Pérez C and others (2019) Fueled by methane: Deep-sea sponges from asphalt seeps gain their nutrition from methane-oxidizing symbionts. *ISME J* 13:1209–1225
- Rubin-Blum M, Makovsky Y, Rahav E, Belkin N, Antler G, Sisma-Ventura G, Herut B (2024) Active microbial communities facilitate carbon turnover in brine pools found in the deep Southeastern Mediterranean Sea. *Mar Environ Res* 198:106497
- ✦ Rubin-Blum M, Rahav E, Sisma-Ventura G, Yudkovski Y and others (2025) Animal burrowing at cold seep ecotones boosts productivity by linking macromolecule turnover with chemosynthesis. *Biogeosciences* 22:1321–1340
- ✦ Rusaouën M, Pujol JP, Bocquet J, Veillard A, Borel JP (1976) Evidence of collagen in the egg capsule of the dogfish, *Scylliorhinus canicula*. *Comp Biochem Physiol B Comp Biochem* 53:539–543
- ✦ Sisma-Ventura G, Bialik OM, Makovsky Y, Rahav E and others (2022) Cold seeps alter the near-bottom biogeochemistry in the ultraoligotrophic Southeastern Mediterranean Sea. *Deep Sea Res I* 183:103744
- ✦ Sisma-Ventura G, Silverman J, Guy-Haim T, Stern N and others (2024) Accumulation of total mercury in deep-sea sediments and biota across a bathymetric gradient in the Southeastern Mediterranean Sea. *Chemosphere* 351:141201
- ✦ Sogin EM, Kleiner M, Borowski C, Gruber-Vodicka HR, Dubilier N (2021) Life in the dark: phylogenetic and physiological diversity of chemosynthetic symbioses. *Annu Rev Microbiol* 75:695–718
- ✦ Stevenson A, Mitchell FJG (2016) Evidence of nutrient partitioning in coexisting deep-sea echinoids, and seasonal dietary shifts in seasonal breeders: perspectives from stable isotope analyses. *Prog Oceanogr* 141:44–59
- ✦ Suh YJ, Ju SJ, Kim MS, Choi H, Shin KH (2023) Trophic diversity of chemosymbiont hosts in deep-sea hydrothermal vents using amino acid nitrogen isotopes. *Front Mar Sci* 10:1204992
- ✦ Toone TA, Washburn TW (2020) Phytodetritus, chemosynthesis, and the dark biosphere: Does depth influence trophic relationships at deep-sea Barbados seeps. *Deep Sea Res I* 165:103367
- ✦ Treude T, Kiel S, Linke P, Peckmann J, Goedert JL (2011) Elasmobranch egg capsules associated with modern and ancient cold seeps: a nursery for marine deep-water predators. *Mar Ecol Prog Ser* 437:175–181
- ✦ van der Meer MTJ, Schouten S, Sinninghe Damsté JS (1998) The effect of the reversed tricarboxylic acid cycle on the ^{13}C contents of bacterial lipids. *Org Geochem* 28:527–533
- ✦ Vokhshoori NL, McCarthy MD, Close HG, Demopoulos AWJ, Prouty NG (2021) New geochemical tools for investigating resource and energy functions at deep-sea cold seeps using amino acid $\delta^{15}\text{N}$ in chemosymbiotic mussels (*Bathymodiolus childressi*). *Geobiology* 19:601–617
- ✦ Wang F, Wu Y, Feng D (2022) Different nitrogen sources fuel symbiotic mussels at cold seeps. *Front Mar Sci* 9:869226
- ✦ Whiteman JP, Elliott Smith EA, Besser AC, Newsome SD (2019) A guide to using compound-specific stable isotope analysis to study the fates of molecules in organisms and ecosystems. *Diversity* 11:8
- ✦ Wickham H (2016) Ggplot2: Elegant graphics for data analysis. Springer International Publishing, Cham
- ✦ Zvi-Kedem T, Shemesh E, Tchernov D, Rubin-Blum M (2021) The worm affair: fidelity and environmental adaptation in symbiont species that co-occur in vestimentiferan tube-worms. *Environ Microbiol Rep* 13:744–752
- ✦ Zvi-Kedem T, Vintila S, Kleiner M, Tchernov D, Rubin-Blum M (2023) Metabolic handoffs between multiple symbionts may benefit the deep-sea bathymodioline mussels. *ISME Commun* 3:48

Editorial responsibility: eroen Ingels,
Wellington, New Zealand

Reviewed by: N. D. Higgs, A. Walters and 1 anonymous referee
Submitted: August 25, 2024; Accepted: January 15, 2025
Proofs received from author(s): March 6, 2025

This article is Open Access under the Creative Commons by Attribution (CC-BY) 4.0 License, <https://creativecommons.org/licenses/by/4.0/deed.en>. Use, distribution and reproduction are unrestricted provided the authors and original publication are credited, and indicate if changes were made